Nuclear Symmetry Energy and the Breaking of the Isospin Symmetry: How Do They Reconcile with Each Other?

X. Roca-Maza* and G. Colò†
Dipartimento di Fisica, Università degli Studi di Milano and INFN, Sezione di Milano, Via Celoria 16, 20133 Milano, Italy

H. Sagawa‡
RIKEN Nishina Center, Wako 351-0198, Japan
and Center for Mathematics and Physics, University of Aizu, Aizu-Wakamatsu, Fukushima 965-8560, Japan

(Received 31 October 2017; revised manuscript received 26 February 2018; published 18 May 2018)

We analyze and propose a solution to the apparent inconsistency between our current knowledge of the equation of state of asymmetric nuclear matter, the energy of the isobaric analog state (IAS) in a heavy nucleus such as ^{208}Pb, and the isospin symmetry breaking forces in the nuclear medium. This is achieved by performing state-of-the-art Hartree-Fock plus random phase approximation calculations of the IAS that include all isospin symmetry breaking contributions. To this aim, we propose a new effective interaction that is successful in reproducing the IAS excitation energy without compromising other properties of finite nuclei.

DOI: 10.1103/PhysRevLett.120.202501

The nuclear physics community has been striving for quite some time to determine the symmetry energy, and in particular, its density dependence [1]. The symmetry energy is the energy per particle needed to change protons into neutrons in uniform matter at a given density ρ. At saturation density of symmetric matter $\rho_0 \approx 0.16$ fm^{-3}, its value is between 29 and 32.7 MeV [2] or between 30.7 and 32.5 MeV [3] if one performs a weighted average of various extractions, but a broader interval, namely, 28.5–34.5 MeV, has been extracted in Ref. [4] (cf. also Ref. [5]). In short, we still do not know precisely the value of the symmetry energy at saturation density, and, as we argue below, its density dependence is even more uncertain.

A deeper understanding would be highly needed because the accurate characterization of the symmetry energy entails profound consequences for the study of the neutron distributions in nuclei along the whole nuclear chart, as well as for other properties of neutron-rich nuclei [1]. Its knowledge impacts heavy-ion reactions where the neutron-proton imbalance varies between the incoming and outgoing interacting nuclei [6]. The symmetry energy is also of paramount importance for understanding the properties of compact objects like neutron stars: it directly impacts, for instance, the determination of the radius of a low-mass neutron star [7], and it is also crucial for understanding stars with a larger mass where the physics of nuclear matter above saturation density also enters. Neutron star physics has received a new strong boost very recently, as the LIGO-Virgo Collaboration announced the first detection of gravitational waves from a binary neutron star merger, setting a new type of constraint on the radius of a neutron star [8]. Neutron star mergers are also a promising site for the r-process nucleosynthesis [9], in which the symmetry energy plays again a substantial role, since the r-process path is governed by the mass of neutron-rich nuclei as well as by their beta decays. Last but not least, the knowledge of the nuclear symmetry energy is relevant for standard model tests via atomic parity violation, as shown, e.g., in Ref. [10].

If β is the local neutron-proton asymmetry $\beta \equiv (\rho_n - \rho_p)/\rho$, the energy per particle (E/A) in matter having neutron-proton imbalance is a function of ρ and β. Such a function can be expanded in even powers of β owing to isospin symmetry (the Coulomb force has to be taken out when dealing with a uniform system). By retaining only the quadratic term, we can write

$$\frac{E}{A}(\rho, \beta) = \frac{E}{A}(\rho, \beta = 0) + S(\rho)\beta^2. \tag{1}$$

This equation defines the symmetry energy $S(\rho)$, that is, the difference between the energy per particle E/A in neutron and symmetric matter. Equation (1) clearly explains why an accurate knowledge of the symmetry energy is mandatory in order to establish a link between the physics of finite nuclei and that of a neutron star.

The symmetry energy can be expanded around saturation density as $S(\rho) = J + L(\rho - \rho_0)/3\rho_0 + ½K_{\rm sym}(\rho - \rho_0)^2/9\rho_0^2 + \cdots$, where different parameters have been defined, namely, $J \equiv S(\rho_0)$, $L \equiv 3\rho_0 S'(\rho_0)$, and $K_{\rm sym} \equiv 9\rho_0^2 S''(\rho_0)$. On these parameters, much attention has been focused. While $K_{\rm sym}$ is basically not known, the error on L referred to as the "slope parameter" is believed to be still significantly larger than the error on J: ranges between 40 and 75 MeV or between 30 and 90 MeV are mentioned in Refs. [2–5]. Many authors have pointed out a correlation between L and the neutron skin $\Delta R_{np} \equiv \langle r_n^2 \rangle^{1/2} - \langle r_p^2 \rangle^{1/2}$ of a heavy nucleus like ^{208}Pb [11–14]. This can be understood also in an intuitive way. The larger the change in symmetry energy as a function of the density, the more convenient the system finds it to push the excess neutrons to a lower density region, that is, toward the surface. Precise and model-independent measurements of the neutron skin are of paramount importance to pin down the value of L [15,16]. Hence, the relevance of experiments like PREX and possible steps forward in the same direction [17–19].

The difficulties in determining the symmetry energy behavior are associated with our still incomplete understanding of the strong interaction in the low-energy regime that is important for nuclei. Then, finding a connection with an observable that is *not* sensitive to the strong force becomes an asset. The isobaric analog state (IAS) is one of the well-established properties of nuclei that is measured accurately, and it is only sensitive to the isospin symmetry breaking (ISB) in the nuclear medium due to Coulomb interaction and, to a lesser extent, the other effects that we will discuss below. Then, here comes the focus of our work. If there is an inconsistency between the properties of the symmetry energy and our knowledge of the IAS and the ISB forces, this is a serious issue. As discussed above, the neutron skin is strongly correlated with the density dependence of the symmetry energy. Therefore, we cannot accept that the values of the neutron skin do not match our understanding of the isospin symmetry, one of the basic symmetries of nature, and of its breaking. In this Letter, a solution is proposed.

Energy density functionals (EDFs) constitute, at present, the only theoretical framework in which the neutron skins and the IAS energies can be consistently calculated from a microscopic perspective in medium-heavy nuclei [20]. Many different parameter sets exist for every class of EDFs; basically, there are three classes of widely used functionals, namely, Skyrme, Gogny, and relativistic mean-field (RMF) functionals. We can focus our attention on some recent accurate functionals and, in particular, on those that have been used in recent years to correlate the symmetry energy parameters with some observables.

Within the Skyrme functionals, SAMi [21] has been shown to be especially accurate in the description of charge-exchange resonances such as the Gamow-Teller resonance. Starting from the prototype SAMi functional, a systematically varied family has been generated by keeping a similar quality of the original fit and varying the values of J and L in Ref. [22]. In addition, a family based also on the systematic variation of J and L with respect to a RMF with density-dependent meson-nucleon (DD-ME [23]) vertices was also introduced. These functionals provide values of the neutron skin through the Hartree-Fock (HF) or Hartree solution for the ground state,

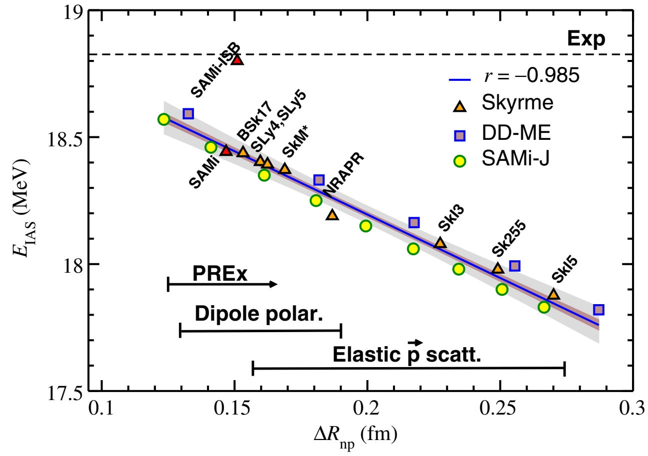

FIG. 1. Energy of the IAS as a function of ΔR_{np}. The arrows indicate the experimental results from polarized proton elastic scattering [26], parity violating elastic electron scattering [18], and from the electric dipole polarizability [27]. See the text for a discussion.

and they provide self-consistently the IAS energy via the charge-exchange random phase approximation (RPA) [24,25]. The results for the IAS energy $E_{\rm IAS}$ as a function of ΔR_{np} are plotted in Fig. 1. For the sake of completeness, the results associated with other Skyrme interactions are also plotted in this figure.

The results displayed in Fig. 1 lie very close to a straight line. This can be understood as follows. The main contribution to $E_{\rm IAS}$ can be evaluated from the Coulomb direct contribution to the so-called displacement energy $\Delta E_d^{C,\rm direct}$ (cf. Ref. [28]). The latter quantity can be approximately calculated by assuming two uniform neutron and proton distributions of radius R_n and R_p, respectively, and approximating the electric charge density with the proton density. This leads to $E_{\rm IAS} \approx \Delta E_d^{C,\rm direct} \approx (6/5)[(Ze^2)/(r_0 A^{1/3})] \times [1-(5/12)^{(1/2)}[N/(N-Z)][(\Delta R_{np})/(r_0 A^{1/3})]]$, where $r_0 = (3/[4\pi\rho_0])^{1/3}$, and, thus, $2r_0$ is the average distance between two nucleons in symmetric nuclear matter at saturation density. For the case of ^{208}Pb, this formula predicts $E_{\rm IAS} \approx 20.9 - 5.7\Delta R_{np}$ (MeV). This result is in qualitative agreement with the linear fit to the microscopic calculations shown in Fig. 1, which gives $E_{\rm IAS} = 19.19(8) - 5.0(2)\Delta R_{np}$ (MeV), with a large correlation coefficient $r = -0.985$. The experimental IAS energy [29] is marked in the figure, and a simple extrapolation of the straight line would imply $\Delta R_{np} = 0.07(2)$ fm. This value is incompatible with many independent analyses [2,5,30]. As a reference, recent experimental constraints from polarized proton elastic scattering [26], parity violating elastic electron scattering [18], and electric dipole polarizability [27] are indicated in the bottom part of Fig. 1.

To solve this puzzle, we have reconsidered all possible contributions to the IAS energy that have *not* been considered with sufficient care in self-consistent calculations so far. All the effects listed below are introduced in the HF mean-field calculations, as one can easily verify that they do not impact the proton-neutron RPA residual force.

1. *Coulomb interaction: Exact direct and exchange contributions*. The Coulomb energy per particle is by far the dominant contribution to the IAS energy. Self-consistent RPA calculations of the IAS are exact, in the specific sense that they preserve the isospin symmetry: if the Coulomb effects are switched completely off, the IAS is found at zero energy [31]. When Skyrme forces are used, it is customary in the literature to adopt the Slater approximation for the Coulomb exchange. In the present case, we have instead included the exact Coulomb exchange. The detailed procedure is explained in Ref. [32], where the reader can also find a detailed analysis for the case of ^{208}Pb. The IAS energy is pushed upwards by ≈100 keV if exact Coulomb exchange is taken into account.

2. *Electromagnetic spin-orbit contribution.* The electromagnetic spin-orbit effect on the single-nucleon energy ε_i is well known and reads [33]

$$\Delta\varepsilon_i = \frac{\hbar^2 c^2}{2m^2 c^4} x_i \langle \vec{l}_i \cdot \vec{s}_i \rangle \int \frac{dr}{r} \frac{dU_{\mathrm{Coul}}}{dr} u_i^2(r), \qquad (2)$$

where $u_i(r)$ is the radial wave function, and x_i is equal to $g_p - 1$ in the case of protons and to g_n in the case of neutrons [$g_n = -3.826\,085\,45(90)$ and $g_p = 5.585\,694\,702(17)$ are the neutron and proton g factors, respectively [34]]. The correction (2) can be estimated to be of the order of tens of keV, and it is basically model independent.

3. *Finite-size effects*. In most of the previous calculations, the Coulomb potential has been evaluated by simply taking into account the point proton density and identifying it with the charge density. In the present work, we have considered in detail all contributions to the charge density which, when written in momentum space up to order $1/m^2$, reads [35]

$$\begin{aligned}\rho_{\mathrm{ch}}(q) = {} & \left(1 - \frac{q^2}{8m^2}\right)[G_{E,p}(q^2)\rho_p(q) + G_{E,n}(q^2)\rho_n(q)] \\ & - \frac{\pi q^2}{2m^2} \sum_{n,l,j,t} [2G_{M,t}(q^2) - G_{E,t}(q^2)] \langle \vec{l} \cdot \vec{s} \rangle \\ & \times \int_0^\infty dr \frac{j_1(qr)}{qr} |u_{n,l,j}(r)|^2, \end{aligned} \qquad (3)$$

where $G_{E,M}$ are the electromagnetic form factors taken from Ref. [36], t labels either protons or neutrons, and the sum runs over the occupied states. Finite-size effects spread out the Coulomb potential: its effects on the p-h excitations that make up the IAS are slightly weaker. The IAS energy decreases, albeit only by a few tens of keV, due to this effect.

TABLE I. Effect of the different contributions from isospin breaking (including both CSB and CIB) mentioned in the text on the IAS energy in ^{208}Pb. Corrections are basically model independent except the last one.

	E_{IAS} (MeV)	Correction (keV)
No corrections	18.31	
Exact Coulomb exchange	18.41	+100
n/p mass difference	18.44	+30
Electromagnetic spin orbit	18.45	+10
Finite-size effects	18.40	−50
Vacuum polarization (V_{ch})	18.53	+130
Isospin symmetry breaking	18.80	+270

4. *Vacuum polarization correction*. From QED, the lowest-order correction to the fine-structure constant or to the Coulomb potential is the vacuum polarization: it amounts to a virtual emission and absorption of an electron-positron pair and produces an extra repulsion that is not completely negligible even at the present low-energy scale. The corresponding potential can be written as follows (cf. Refs. [37,38] and Ref. [39] in the case of a finite-size particle):

$$V_{\mathrm{VP}}(\vec{r}) = \frac{2}{3} \frac{\alpha e^2}{\pi} \int d\vec{r}' \frac{\rho(\vec{r}')}{|\vec{r} - \vec{r}'|} \mathcal{K}_1 \left(\frac{2}{\lambda\!\!\!^{-}_e} |\vec{r} - \vec{r}'| \right), \qquad (4)$$

where α is the fine-structure constant, $\lambda\!\!\!^{-}_e$ the reduced Compton electron wavelength, and

$$\mathcal{K}_1(x) \equiv \int_1^\infty dt e^{-xt} \left(\frac{1}{t^2} + \frac{1}{2t^4} \right) \sqrt{t^2 - 1}. \qquad (5)$$

5. *Charge-symmetry-breaking and charge-independence-breaking forces*. The contributions (1)–(4) together with the n-p mass difference, which is one of the charge-symmetry-breaking (CSB) potential terms, produce an overall upward shift of the IAS energy, and the same for the straight line that connects the points of Fig. 1. In Table I, we can see that this shift, by adding also the small effect of the neutron-proton mass difference, amounts to ≈220 keV, and, consequently, it is too small in order to let the line intersect the experimental value for the IAS energy at a point that corresponds to a realistic range of ΔR_{np} (indicated by the horizontal bars in Fig. 1).

CSB and charge-independence-breaking (CIB) effects have been widely discussed in the literature (see, for example, Refs. [40–42]); however, most of the efforts have been devoted to study their impact on few-nucleon systems and few-hadron systems or to derive them from QCD through effective field theory methods. Recently, the isospin mixing in ^{8}Be was studied based on the Green's function Monte Carlo method by including the CSB interaction [43]. Although it has been known for many

TABLE II. SAMi-ISB parameter set. The statistical errors σ are given in parentheses. See text for details.

	Value (σ)		Value (σ)
t_0	−2098.3(149.3) MeV fm^3	x_0	0.242(9)
t_1	394.7(15.8) MeV fm^5	x_1	−0.17(33)
t_2	−136.4(10.8) MeV fm^5	x_2	−0.470(4)
t_3	11 995(686) MeV fm$^{3+3\alpha}$	x_3	0.32(21)
W_0	294(6)		
W_0'	−367(12)	s_0	−26.3(7) MeV fm^3
α	0.223(31)	u_0	25.8(4) MeV fm^3

years that CSB and CIB forces must be taken into account to reproduce the so-called Nolen-Schiffer anomaly along the nuclear chart, the information on CSB and CIB forces in the nuclear medium is scarce. The nuclear shell model has been employed for quite some time to analyze the energies along the isobaric multiplets; recently, long sequences of multiplets in rotational bands have been used to determine the magnitude of CSB and CIB effects [44]. In the same context, it has been noticed that CSB and CIB interactions needed to explain the data are not consistent with those in vacuum [45]. Similar conclusions have been drawn in Ref. [46].

Therefore, in the present work, we have kept our description simple and aimed to reconcile the scarce information about CSB and CIB in the medium, and the reproduction of the IAS energy, with a realistic value for the neutron skin. Borrowing from Ref. [47] [cf. Eqs. (18)–(21)], we define simpler Skyrme-like CSB and CIB interactions as follows:

$$V_{\mathrm{CSB}}(\vec{r}_1,\vec{r}_2) \equiv \frac{1}{4}[\tau_z(1)+\tau_z(2)]s_0(1+y_0P_\sigma)\delta(\vec{r}_1-\vec{r}_2),$$

and

$$V_{\mathrm{CIB}}(\vec{r}_1,\vec{r}_2) \equiv \frac{1}{2}\tau_z(1)\tau_z(2)u_0(1+z_0P_\sigma)\delta(\vec{r}_1-\vec{r}_2).$$

P_σ is the spin-exchange operator and we take $y_0 = -1$ and $z_0 = -1$. The momentum-dependent terms written in Ref. [47] have not been considered under the rationale that the information that we have at our disposal is not sufficient to pin down the values of all parameters of a general interaction with several partial waves.

We have looked at the ISB contributions to the energy per particle of symmetric nuclear matter, as predicted by the Brueckner-Hartree-Fock calculations of Ref. [48] (based on AV18 [49]). We have determined a new Skyrme parameter set named SAMi-ISB using the same fitting protocol of SAMi but including CSB and CIB contributions [50]. We have first started from existing parameters of SAMi and fixed the values of s_0 and u_0 by requiring a reproduction of the results of Ref. [48] and the value of the IAS energy in

TABLE III. Experimental data [57,58] and SAMi-ISB results for the binding energies (B), charge radii (r_c), and neutron skin thickness (ΔR_{np}) for some selected nuclei.

Element	N	B (MeV)	B^{exp} (MeV)	r_c (fm)	r_c^{exp} (fm)	ΔR_{np} (fm)
Ca	28	417.67	415.99	3.49	3.47	0.214
Zr	50	783.60	783.89	4.26	4.27	0.097
Sn	82	1102.75	1102.85	4.73	$(\cdots)$	0.217
Pb	126	1635.78	1636.43	5.50	5.50	0.151

^{208}Pb. This gives [the adopted deviations that lead to the estimated statistical errors are 30 keV on the IAS energy and 10 keV ($\sim$10% error) on the CSB contribution to E/A in symmetric matter] $s_0 = -26.3(7)$ MeV fm^3 and $u_0 = 25.8(4)$ MeV fm^3. Then, the standard Skyrme parameters have been refitted; the effect of CSB or CIB is included, but these forces affect the binding energies and charge radii only by a few per mil or percent, so that this two-step strategy is feasible.

The values of the SAMi-ISB parameters are provided in Table II. As seen in Fig. 1, with SAMi-ISB, the IAS energy of ^{208}Pb is predicted at $E_{\mathrm{IAS}} = 18.80(5)$ MeV ($E_{\mathrm{IAS}}^{\mathrm{exp}} = 18.826 \pm 0.010$ MeV [29]) with the neutron skin $\Delta R_{np} = 0.151(7)$ fm, which is within the realistic range deduced from the three experiments. The quality of this interaction is similar or better than SAMi if we look at the overall properties like those in uniform matter. The values of J and L are, in the case of SAMi-ISB (SAMi), 30.8(4) MeV (28(1) MeV) and 50(4) MeV (44(7) MeV). These are quite realistic values according to our general discussion at the start of this Letter. While the detailed assessment of SAMi-ISB along the isotope chart is out of our scope here, we show in Table III some results for binding energies, charge radii, and neutron skin thicknesses. Moreover, we have checked the predictive power of SAMi-ISB by calculating the IAS energy in other nuclei. In the Sn isotopes with $A = 112$–124, the IAS energies calculated with SAMi differ from the experimental values by about 600 keV, while this discrepancy is reduced to $\approx$50–200 keV by using SAMi-ISB. In ^{40}Ca and ^{90}Zr, the results obtained with SAMi-ISB are also improved with respect to SAMi [50].

In conclusion, SAMi-ISB is a new parametrization of a Skyrme-like EDF that reconciles standard nuclear properties (saturation density, binding energy, and charge radii of finite nuclei) with *both* our current understanding of the density behavior of the symmetry energy *and* the reproduction of the IAS energy of ^{208}Pb as well as in Sn isotopes. We have self-consistently included for the first time within the HF + RPA framework all known contributions that break the isospin symmetry. All of these contributions have been calculated in a model-independent way, except the CSB and CIB contribution. We have fixed only two free parameters in the CSB and CIB terms, and we have shown that this allows reproducing at the same time BHF calculations based on AV18, and the IAS energy of a heavy nucleus such as ^{208}Pb without compromising the other properties of nuclear matter and finite nuclei.

Funding from the European Union's Horizon 2020 research and innovation program under Grant No. 654002 is acknowledged. We would like to kindly thank Prof. K. Neergård for a careful reading of the manuscript and for useful comments.

*xavier.roca.maza@mi.infn.it
†colo@mi.infn.it
‡hiroyuki.sagawa@gmail.com

[1] B.-A. Li, À. Ramos, G. Verde, and I. E. Vidaña, Eur. Phys. J. A **50**, 9 (2014).
[2] J. M. Lattimer and Y. Lim, Astrophys. J. **771**, 51 (2013).
[3] B.-A. Li and X. Han, Phys. Lett. B **727**, 276 (2013).
[4] M. Oertel, M. Hempel, T. Klähn, and S. Typel, Rev. Mod. Phys. **89**, 015007 (2017).
[5] C. J. Horowitz, E. F. Brown, Y. Kim, W. G. Lynch, R. Michaels, A. Ono, J. Piekarewicz, M. B. Tsang, and H. H. Wolter, J. Phys. G **41**, 093001 (2014).
[6] M. Tsang, Z. Chajecki, D. Coupland, P. Danielewicz, F. Famiano, R. Hodges, M. Kilburn, F. Lu, W. Lynch, J. Winkelbauer, M. Youngs, and Y. Zhang, Prog. Part. Nucl. Phys. **66**, 400 (2011).
[7] J. Carriere, C. J. Horowitz, and J. Piekarewicz, Astrophys. J. **593**, 463 (2003).
[8] B. P. Abbott, R. Abbott, T. D. Abbott, F. Acernese, K. Ackley, C. Adams, T. Adams, P. Addesso, and R. X. Adhikari (LIGO Scientific Collaboration and Virgo Collaboration), Phys. Rev. Lett. **119**, 161101 (2017).
[9] D. Kasen, B. Metzger, J. Barnes, E. Quataert, and E. Ramirez-Ruiz, Nature (London) **551**, 80 (2017).
[10] T. Sil, M. Centelles, X. Viñas, and J. Piekarewicz, Phys. Rev. C **71**, 045502 (2005).
[11] B. A. Brown, Phys. Rev. Lett. **85**, 5296 (2000).
[12] S. Typel and B. A. Brown, Phys. Rev. C **64**, 027302 (2001).
[13] R. Furnstahl, Nucl. Phys. **706A**, 85 (2002).
[14] M. Centelles, X. Roca-Maza, X. Viñas, and M. Warda, Phys. Rev. Lett. **102**, 122502 (2009).
[15] X. Roca-Maza, M. Centelles, X. Viñas, and M. Warda, Phys. Rev. Lett. **106**, 252501 (2011).
[16] B. A. Brown, Phys. Rev. Lett. **119**, 122502 (2017).
[17] S. Abrahamyan *et al.* (PREX Collaboration), Phys. Rev. Lett. **108**, 112502 (2012).
[18] C. J. Horowitz, Z. Ahmed, C.-M. Jen, A. Rakhman, P. A. Souder, M. M. Dalton, N. Liyanage, K. D. Paschke, K. Saenboonruang, R. Silwal, G. B. Franklin, M. Friend, B. Quinn, K. S. Kumar, D. McNulty, L. Mercado, S. Riordan, J. Wexler, R. W. Michaels, and G. M. Urciuoli, Phys. Rev. C **85**, 032501 (2012).
[19] C. J. Horowitz, K. S. Kumar, and R. Michaels, Eur. Phys. J. A **50**, 48 (2014).
[20] M. Bender, P.-H. Heenen, and P.-G. Reinhard, Rev. Mod. Phys. **75**, 121 (2003).
[21] X. Roca-Maza, G. Colò, and H. Sagawa, Phys. Rev. C **86**, 031306 (2012).
[22] X. Roca-Maza, M. Brenna, B. K. Agrawal, P. F. Bortignon, G. Colò, L.-G. Cao, N. Paar, and D. Vretenar, Phys. Rev. C **87**, 034301 (2013).
[23] D. Vretenar, T. Nikšić, and P. Ring, Phys. Rev. C **68**, 024310 (2003).
[24] G. Colò, N. Van Giai, P. F. Bortignon, and R. A. Broglia, Phys. Rev. C **50**, 1496 (1994).
[25] N. Paar, T. Nikšić, D. Vretenar, and P. Ring, Phys. Rev. C **69**, 054303 (2004).
[26] J. Zenihiro, H. Sakaguchi, T. Murakami, M. Yosoi, Y. Yasuda, S. Terashima, Y. Iwao, H. Takeda, M. Itoh, H. P. Yoshida, and M. Uchida, Phys. Rev. C **82**, 044611 (2010).
[27] X. Roca-Maza, X. Viñas, M. Centelles, B. K. Agrawal, G. Colò, N. Paar, J. Piekarewicz, and D. Vretenar, Phys. Rev. C **92**, 064304 (2015).
[28] N. Auerbach, J. Hüfner, A. K. Kerman, and C. M. Shakin, Phys. Rev. Lett. **23**, 484 (1969).
[29] M. Martin, Nucl. Data Sheets **108**, 1583 (2007).
[30] X. Viñas, M. Centelles, X. Roca-Maza, and M. Warda, Eur. Phys. J. A **50**, 27 (2014).
[31] C. A. Engelbrecht and R. H. Lemmer, Phys. Rev. Lett. **24**, 607 (1970).
[32] X. Roca-Maza, L.-G. Cao, G. Colò, and H. Sagawa, Phys. Rev. C **94**, 044313 (2016).
[33] *Isospin in Nuclear Physics*, edited by D. Wilkinson (North-Holland, Amsterdam, 1967).
[34] P. J. Mohr, D. B. Newell, and B. N. Taylor, Rev. Mod. Phys. **88**, 035009 (2016).
[35] L. Ray, Phys. Rev. C **19**, 1855 (1979).
[36] J. Friedrich and T. Walcher, Eur. Phys. J. A **17**, 607 (2003).
[37] E. A. Uehling, Phys. Rev. **48**, 55 (1935).
[38] J. Schwinger, Phys. Rev. **75**, 651 (1949).
[39] L. W. Fullerton and G. A. Rinker, Phys. Rev. A **13**, 1283 (1976).
[40] E. M. Henley and G. A. Miller, in *Mesons in Nuclei*, edited by M. Rho and D. H. Wilkinson (North-Holland, Amsterdam, 1979).
[41] G. A. Miller, B. M. K. Nefkens, and I. Slaus, Phys. Rep. **194**, 1 (1990).
[42] U. van Klock, J. L. Friar, and T. Goldmann, Phys. Lett. B **371**, 169 (1996).
[43] R. B. Wiringa, S. Pastore, S. C. Pieper, and G. A. Miller, Phys. Rev. C **88**, 044333 (2013).
[44] M. Bentley and S. Lenzi, Prog. Part. Nucl. Phys. **59**, 497 (2007).
[45] M. A. Bentley, S. M. Lenzi, S. A. Simpson, and C. A. Diget, Phys. Rev. C **92**, 024310 (2015).
[46] P. Baczyk, J. Dobaczewski, M. Konieczka, W. Satula, T. Nakatsukasa, and K. Sato, Phys. Lett. B **778**, 178 (2018).
[47] H. Sagawa, N. V. Giai, and T. Suzuki, Phys. Lett. B **353**, 7 (1995).
[48] H. Muther, A. Polls, and R. Machleidt, Phys. Lett. B **445**, 259 (1999).
[49] R. B. Wiringa, V. G. J. Stoks, and R. Schiavilla, Phys. Rev. C **51**, 38 (1995).
[50] See Supplemental Material at http://link.aps.org/supplemental/10.1103/PhysRevLett.120.202501 for a description of some technical details on the Hartree-Fock

plus random phase approximation calculations reported here, on the fitting protocol, and the covariance analysis of the newly introduced interaction SAMi-ISB. E_{IAS} predictions for some selected nuclei are also given. This material contains Refs. [21,24,32,48,49,51–56].

[51] X. Roca-Maza, N. Paar, and G. Colò, J. Phys. G **42**, 034033 (2015).

[52] M. Kortelainen, T. Lesinski, J. Moré, W. Nazarewicz, J. Sarich, N. Schunck, M. V. Stoitsov, and S. Wild, Phys. Rev. C **82**, 024313 (2010).

[53] G. Colò, L. Cao, N. V. Giai, and L. Capelli, Comput. Phys. Commun. **184**, 142 (2013).

[54] F. James, *Minuit Function Minimization and Error Analysis: Reference Manual Version 94.1* (CERN Program Library Long Writeup D506, Geneva, Switzerland, 1994).

[55] E. Chabanat, P. Bonche, P. Haensel, J. Meyer, and R. Schaeffer, Nucl. Phys. **627A**, 710 (1997).

[56] M. Antony, A. Pape, and J. Britz, At. Data Nucl. Data Tables **66**, 1 (1997).

[57] W. Huang, G. Audi, M. Wang, F. Kondev, S. Naimi, and X. Xu, Chin. Phys. C **41**, 030002 (2017).

[58] I. Angeli and K. Marinova, At. Data Nucl. Data Tables **99**, 69 (2013).